Cross-relaxation dynamics of the N-V center in diamond as studied via optically detected microwave recovery transients

I. Hiromitsu,* J. Westra, and M. Glasbeek
Laboratory for Physical Chemistry, University of Amsterdam, Nieuwe Achtergracht 127, 1018 WS, Amsterdam, The Netherlands
(Received 11 February 1992)

The N-V center in diamond is a nitrogen-vacancy pair defect with an electronic triplet spin ground state. Upon optical excitation and in the presence of an applied magnetic field, two subensembles of N-V centers with different spin temperatures are created at liquid-helium temperatures. For certain magnetic fields, magnetically inequivalent N-V centers become resonant and the subensembles comprising these N-V centers tend to equilibrate due to cross relaxation. In this paper the dynamics of the cross-relaxation process is studied by means of optical-microwave double-resonance techniques. Pulsed microwave excitation of the ground-state spin transitions appears to produce a transient behavior of the optically induced fluorescence. A detailed kinetic analysis is given showing that the recovery rates obtained for a series of laser excitation powers, when extrapolated to zero excitation power, yield the cross-relaxation rate constant. The rate constant for cross relaxation among magnetically inequivalent N-V centers is found to be $(2.0\pm0.3)\times10^2$ s^{-1}, whereas cross relaxation with doublet electron-spin species in the lattice occurs with a rate of $(9.1\pm1.4)\times10^2$ s^{-1}.

I. INTRODUCTION

Cross relaxation (CR) of electron spins is an energy-exchange process involving mutual flip-flops between distant spins.[1,2] As a result of cross relaxation, a common spin temperature can be achieved within the system of localized spins. Thus, in order to understand the spin thermodynamics of the system, it is important to understand the details of the CR process. In a few recent papers,[3,4] CR dynamics of N-V centers in a diamond crystal has been studied by means of optically detected spin coherent transient measurements. The N-V center in diamond is a defect consisting of a substitutional nitrogen atom adjacent to a carbon-atom vacancy.[5-7] In optically detected spin-locking,[8] optical hole-burning,[9] and nearly degenerate four-wave mixing[10] studies of the N-V center, it was shown that the ground state of the N-V center is an electron-spin triplet state. The spin Hamiltonian parameters that characterize this triplet state are $g=2.00$, $|D|=2880$ MHz, and $|E|=0$ MHz. The defect has axial local symmetry. The principal axis of the fine-structure tensor is along a [111] crystallographic direction (cf. Fig. 1).

In the presence of an externally applied magnetic field along the [111] axis, sudden changes in the intensity of the N-V center emission, as detected at the zero-phonon wavelength of 638 nm, have been observed for magnetic-field strengths of 514 and 600 G.[3] Analysis of the anisotropic behavior of the emission intensity changes showed that at a magnetic field of 600 G the fluorescence intensity changes are due to CR between magnetically inequivalent N-V centers, whereas CR with an electron-spin doublet system accounts for the intensity changes in a magnetic field of 514 G. Also, at zero magnetic field, all N-V centers are resonant and CR involving all N-V center sites occurs.[3,4] Under conditions of CR between magnetically inequivalent N-V centers, spin coherent transients as measured in Hahn echo decay (HED), stimulated echo decay (SED), and spin-locking echo decay (SLD) experiments were found[3,4] to be enhanced by a factor of 2.0, 3.0, and 2.2, respectively. The results could be explained on the basis of magnetic dipole-dipole couplings between the N-V center triplet spins in the different subensembles.

In the present study, the dynamics of CR of the N-V center triplet spins is examined by means of time-resolved microwave recovery experiments performed for the N-V center in diamond. In these incoherent transient experiments, after an initial microwave pulse has induced a spin transition in the triplet ground state while at the same

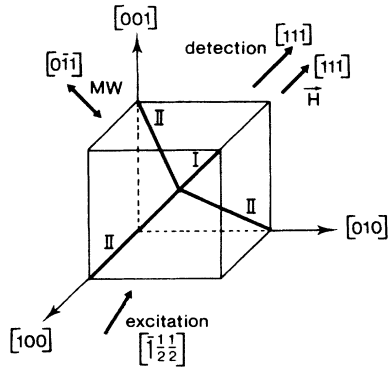

FIG. 1. Orientation of the molecular main axes of the N-V centers in subensembles I and II with respect to the diamond crystallographic axes. Directions relevant to the present microwave recovery experiments are shown. MW indicates the direction of the linearly polarized microwave magnetic-field component.

time maintaining cw optical excitation of the N-V center, the recovery of the optical emission intensity of the N-V center is measured as a function of time. Generally, the microwave recovery kinetics is determined by the population relaxation of the spin levels, while for the spin echo the decay rates are determined by pure spin dephasing as well as population relaxation processes. In this paper it will be discussed that the CR dynamics as determined in the microwave recovery experiments for the N-V center in diamond is representative of the mean flip-flop rate of each N-V center spin. On the other hand, the CR dynamics probed in the coherent transient experiments reported previously[3,4] provides information concerning the local-field fluctuations produced by the entire collection of distant flip-flopping spins. In Sec. II it is analyzed how for the N-V center the ground-state triplet spin kinetics is affected by the CR in zero magnetic field. The treatment is analogous to that introduced recently for the analysis of the CR results of the 2.818-eV center in diamond in the photoexcited triplet state.[11] The CR kinetics of the N-V center discussed in this paper, however, differs considerably from the analysis presented for the CR kinetics of the 2.818-eV center. Basically, the differences arise from the fact that the N-V center has a triplet ground state, whereas the 2.818-eV center has a photoexcited triplet state. As will be shown later, several new aspects appear in the CR process for the N-V center in diamond. Here we mention the following: (i) the depletion of the triplet-state population of the N-V centers by optical excitation cannot be neglected in the kinetic analysis; this is in contrast to previous results for the 2.818-eV center;[11] (ii) the polarization of the excitation light is of fundamental importance for observing CR for the N-V center; (iii) CR occurs because of dipolar interactions between subensembles of N-V centers with different spin temperatures, whereas for the 2.818-eV center the optically induced spin alignment was relaxed by contact with optically inactive spin species; and (iv) the CR process for the N-V center is examined in zero magnetic field and in the limit of zero excitation power, whereas for the 2.818-eV center CR can only be observed in the presence of a magnetic field. The experimental part is presented in Sec. III. In Sec. IV the results of the microwave recovery transient measurements and the CR rates as estimated on the basis of the analysis of Sec. II are presented. The estimated CR rates are in the order of 10^2–10^3 s^{-1}. By contrast, the CR effects on the spin dephasing rates are of the order of 10^3–10^4 s^{-1}.[3,4] A qualitative explanation of the difference between the microwave recovery and spin coherence results is presented in Sec. V.

II. ANALYSIS OF GROUND-STATE TRIPLET SPIN KINETICS FOR THE N-V CENTER

A. CR for N-V centers at zero magnetic field

In zero magnetic field, all N-V centers in diamond possess identical magnetic-resonance frequencies and CR occurs between them. When a magnetic field is applied along the crystallographic [111] axis, the N-V centers are divided into two magnetically inequivalent subensembles I and II. N-V centers belonging to subensemble I have their molecular main axis along the [111] direction (i.e., the direction of the external magnetic field), while the N-V centers belonging to subensemble II have their molecular main axis along either the $[1\,\bar{1}\,\bar{1}]$, $[\bar{1}\,1\,\bar{1}]$, or $[\bar{1}\,\bar{1}\,1]$ axis (cf. Fig. 1). Although the two subensembles are magnetically equivalent at zero magnetic field, a distinction between the two subensembles can still be made because of their different optical excitation rates when the polarization of the excitation light is along the [111] crystallographic axis. This point is thoroughly discussed in Secs. IV A and IV B. Another feature of the N-V center at zero magnetic field is that two of the three triplet sublevels are degenerate ($|E|=0$).

We consider a model consisting of three energy levels for each subensemble, i.e., ground-state triplet sublevels $T_1^{\rm I}$ (or $T_1^{\rm II}$) and $T_2^{\rm I}$ ($T_2^{\rm II}$) and an excited state $T_*^{\rm I}$ ($T_*^{\rm II}$), the sublevel $T_1^{\rm I}$ ($T_1^{\rm II}$) being doubly degenerate. In Fig. 2(a) the optical excitation and decay rate constants of the triplet state are defined for the two subensembles I and II: $k_1^{\rm I}$ (or $k_1^{\rm II}$) ($i=1,2$) represents the excitation rate of the triplet sublevel $T_1^{\rm I}$ ($T_1^{\rm II}$), and $A_1^{\rm I}$ ($A_1^{\rm II}$) represents the decay rate of the excited state $T_*^{\rm I}$ ($T_*^{\rm II}$) into the ground-state sublevel $T_1^{\rm I}$ ($T_1^{\rm II}$). Since the energy difference between the sublevels $T_1^{\rm I}$ and $T_2^{\rm I}$ is resonant with the energy difference between the sublevels $T_1^{\rm II}$ and $T_2^{\rm II}$, CR occurs between the two subensembles. The CR is expressed by the rate equation[12,13]

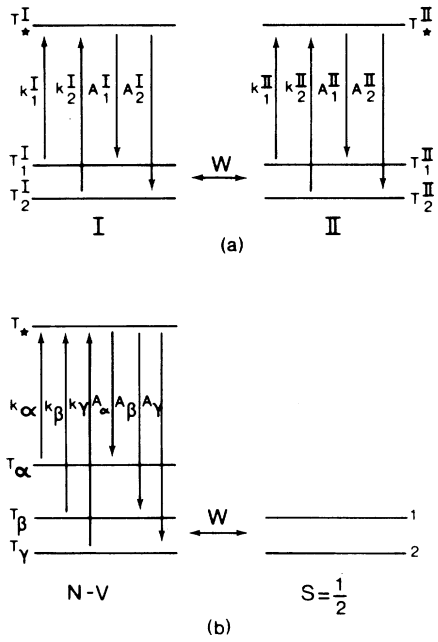

FIG. 2. (a) Schematic representation of the energy levels of N-V centers in subensembles I and II at zero external magnetic field. The $T_2^{\rm I} \rightarrow T_1^{\rm I}$ sublevel transitions are resonant to each other. (b) The energy levels of N-V centers in subensemble I and a doublet species under external magnetic field. The doublet species is resonant to the $T_\gamma \rightarrow T_\beta$ sublevel transition.

$$\frac{dN_1^{\mathrm{I}}}{dt}=-W'(N_1^{\mathrm{I}}N_2^{\mathrm{II}}-N_2^{\mathrm{I}}N_1^{\mathrm{II}}) , \tag{1}$$

where N_1^{I} (or N_1^{II}) ($i=1,2$) represents the population of the ground-state triplet sublevel T_1^{I} (T_1^{II}) and W' represents the CR rate. It is known that under continuous optical excitation at liquid-helium temperatures, N-V centers exhibit spin alignment,[3] e.g., $N_1^{\mathrm{I}}>N_2^{\mathrm{I}}$ or $N_1^{\mathrm{I}}<N_2^{\mathrm{I}}$. However, as will be explained later in this section, our main interest is in the case of excitation at low laser powers, such that the excitation rates become smaller than the CR rate. In this case there is little spin alignment, and a high-temperature approximation is applicable for Eq. (1). We write

$$\begin{aligned}\frac{dN_1^{\mathrm{I}}}{dt}&=-\frac{W'}{2}\{N^{\mathrm{II}}(N_1^{\mathrm{I}}-N_2^{\mathrm{I}})-N^{\mathrm{I}}(N_1^{\mathrm{II}}-N_2^{\mathrm{II}})\}\\&=-\frac{W}{2}\{(N_1^{\mathrm{I}}-N_2^{\mathrm{I}})-\frac{1}{p}(N_1^{\mathrm{II}}-N_2^{\mathrm{II}})\} ,\end{aligned} \tag{2}$$

where N^{I} and N^{II} are the total number of N-V centers belonging to the subensembles I and II, respectively, and p is defined as $p=N^{\mathrm{II}}/N^{\mathrm{I}}$, which takes a value of 3 in the present case. In Eq. (2) the CR rate W is defined as

$$W=\frac{N^{\mathrm{II}}}{2}W' . \tag{3}$$

Neglecting spin-lattice relaxation, the rate equations for the populations of the six energy levels become

$$\begin{aligned}\frac{dN_*^{\mathrm{I}}}{dt}&=k_1^{\mathrm{I}}N_1^{\mathrm{I}}+k_2^{\mathrm{I}}N_2^{\mathrm{I}}-(A_1^{\mathrm{I}}+A_2^{\mathrm{I}})N_*^{\mathrm{I}} ,\\
\frac{dN_*^{\mathrm{II}}}{dt}&=k_1^{\mathrm{II}}N_1^{\mathrm{II}}+k_2^{\mathrm{II}}N_2^{\mathrm{II}}-(A_1^{\mathrm{II}}+A_2^{\mathrm{II}})N_*^{\mathrm{II}} ,\\
\frac{dN_1^{\mathrm{I}}}{dt}&=-k_1^{\mathrm{I}}N_1^{\mathrm{I}}+A_1^{\mathrm{I}}N_*^{\mathrm{I}}\\&\quad-\frac{W}{2}\{(N_1^{\mathrm{I}}-N_2^{\mathrm{I}})-\frac{1}{p}(N_1^{\mathrm{II}}-N_2^{\mathrm{II}})\} ,\\
\frac{dN_2^{\mathrm{I}}}{dt}&=-k_2^{\mathrm{I}}N_2^{\mathrm{I}}+A_2^{\mathrm{I}}N_*^{\mathrm{I}}\\&\quad+\frac{W}{2}\{(N_1^{\mathrm{I}}-N_2^{\mathrm{I}})-\frac{1}{p}(N_1^{\mathrm{II}}-N_2^{\mathrm{II}})\} ,\\
\frac{dN_1^{\mathrm{II}}}{dt}&=-k_1^{\mathrm{II}}N_1^{\mathrm{II}}+A_1^{\mathrm{II}}N_*^{\mathrm{II}}\\&\quad+\frac{W}{2}\{(N_1^{\mathrm{I}}-N_2^{\mathrm{I}})-\frac{1}{p}(N_1^{\mathrm{II}}-N_2^{\mathrm{II}})\} ,\\
\frac{dN_2^{\mathrm{II}}}{dt}&=-k_2^{\mathrm{II}}N_2^{\mathrm{II}}+A_2^{\mathrm{II}}N_*^{\mathrm{II}}\\&\quad-\frac{W}{2}\{(N_1^{\mathrm{I}}-N_2^{\mathrm{I}})-\frac{1}{p}(N_1^{\mathrm{II}}-N_2^{\mathrm{II}})\} ,\end{aligned} \tag{4}$$

where N_*^{I} (or N_*^{II}) is the population of the excited state T_*^{I} (T_*^{II}). Additional conditions are

$$\begin{aligned}N_1^{\mathrm{I}}+N_2^{\mathrm{I}}+N_*^{\mathrm{I}}&=N^{\mathrm{I}} ,\\
N_1^{\mathrm{II}}+N_2^{\mathrm{II}}+N_*^{\mathrm{II}}&=N^{\mathrm{II}} .\end{aligned} \tag{5}$$

Equation (5) reduces the number of independent variables to 4.

Since the order of the decay rates,[14] e.g., A_1^{I}, is $10^8\ \mathrm{s}^{-1}$ and that of the excitation rates, e.g., k_1^{I}, is 10^2–$10^3\ \mathrm{s}^{-1}$ with the present laser intensity, the populations of the excited states, e.g., N_*^{I}, are five to six orders of magnitude smaller than the ground-state populations, e.g., N_1^{I}. Because of this large difference, Eq. (4) can be solved analytically. For simplicity, we assume

$$A_1^{\mathrm{I}}=\alpha A_2^{\mathrm{I}},\quad A_1^{\mathrm{II}}=\alpha A_2^{\mathrm{II}} , \tag{6}$$

where α is a constant. The four variables N_*^{I}, N_*^{II}, $n=N_1^{\mathrm{I}}-\alpha N_2^{\mathrm{I}}$, and $m=N_1^{\mathrm{II}}-\alpha N_2^{\mathrm{II}}$ are chosen as the four independent variables. Neglecting small terms such as $k_1^{\mathrm{I}}N_*^{\mathrm{I}}$, which are five to six orders of magnitude smaller than terms such as $k_1^{\mathrm{I}}N_1^{\mathrm{I}}$ or $A_1^{\mathrm{I}}N_*^{\mathrm{I}}$, the rate equations for the four variables become

$$\frac{d}{dt}\bar{a}=\bar{A}-R\bar{a} , \tag{7}$$

where

$$\bar{a}=\begin{pmatrix}N_*^{\mathrm{I}}\\N_*^{\mathrm{II}}\\n\\m\end{pmatrix},\quad \bar{A}=\begin{pmatrix}\{K_1^{\mathrm{I}}+(\alpha-1)K_2^{\mathrm{I}}\}N^{\mathrm{I}}\\\{K_1^{\mathrm{II}}+(\alpha-1)K_2^{\mathrm{II}}\}N^{\mathrm{II}}\\-\alpha K_2^{\mathrm{I}}N^{\mathrm{I}}\\-\alpha K_2^{\mathrm{II}}N^{\mathrm{II}}\end{pmatrix}$$

and

$$R=\begin{pmatrix}A_1^{\mathrm{I}}+A_2^{\mathrm{I}}&0&-K_2^{\mathrm{I}}&0\\0&A_1^{\mathrm{II}}+A_2^{\mathrm{II}}&0&-K_2^{\mathrm{II}}\\0&0&K_1^{\mathrm{I}}+W&-W/p\\0&0&-W&K_1^{\mathrm{II}}+W/p\end{pmatrix} .$$

In Eq. (7), K_1^{I}, K_2^{I}, K_1^{II}, and K_2^{II} are defined as

$$\begin{aligned}K_1^{\mathrm{I}}&=\frac{k_1^{\mathrm{I}}+\alpha k_2^{\mathrm{I}}}{1+\alpha},\quad K_2^{\mathrm{I}}=\frac{k_1^{\mathrm{I}}-k_2^{\mathrm{I}}}{1+\alpha} ,\\
K_1^{\mathrm{II}}&=\frac{k_1^{\mathrm{II}}+\alpha k_2^{\mathrm{II}}}{1+\alpha},\quad K_2^{\mathrm{II}}=\frac{k_1^{\mathrm{II}}-k_2^{\mathrm{II}}}{1+\alpha} .\end{aligned} \tag{8}$$

The four eigenvalues of the matrix R are

$$\begin{aligned}&\lambda_1=A_1^{\mathrm{I}}+A_2^{\mathrm{I}},\quad \lambda_2=A_1^{\mathrm{II}}+A_2^{\mathrm{II}} ,\\
&\lambda_\pm=\tfrac{1}{2}\left[K_1^{\mathrm{I}}+K_1^{\mathrm{II}}+\left[1+\frac{1}{p}\right]W\right.\\&\qquad\left.\pm\left[\left\{K_1^{\mathrm{I}}-K_1^{\mathrm{II}}+\left[1-\frac{1}{p}\right]W\right\}^2+4W^2/p\right]^{1/2}\right] .\end{aligned} \tag{9}$$

Since the emission intensities from the two subensembles I and II are proportional to $(A_1^{\mathrm{I}}+A_2^{\mathrm{I}})N_*^{\mathrm{I}}$ and $(A_1^{\mathrm{II}}+A_2^{\mathrm{II}})N_*^{\mathrm{II}}$, respectively, we need to obtain the solutions for N_*^{I} and N_*^{II}, which are

$$\begin{aligned}N_*^{\mathrm{I}}(t)-N_*^{\mathrm{I}}(\infty)&=E_1^{\mathrm{I}}e^{-\lambda_1 t}-E_+^{\mathrm{I}}e^{-\lambda_+ t}-E_-^{\mathrm{I}}e^{-\lambda_- t} ,\\
N_*^{\mathrm{II}}(t)-N_*^{\mathrm{II}}(\infty)&=E_2^{\mathrm{II}}e^{-\lambda_2 t}-E_+^{\mathrm{II}}e^{-\lambda_+ t}-E_-^{\mathrm{II}}e^{-\lambda_- t} ,\end{aligned} \tag{10}$$

where

$$E_+^{\mathrm{I}}=\frac{K_2^{\mathrm{I}}W/p}{(Q^2+W^2/p)\lambda_1}C_+ ,$$

$$E_-^{\mathrm{I}}=\frac{K_2^{\mathrm{I}}Q}{(Q^2+W^2/p)\lambda_1}C_- ,$$

$$E_+^{\mathrm{II}}=-\frac{K_2^{\mathrm{II}}Q}{(Q^2+W^2/p)\lambda_2}C_+ ,$$

$$E_-^{\mathrm{II}}=\frac{K_2^{\mathrm{II}}W}{(Q^2+W^2/p)\lambda_2}C_- ,$$

with $Q=\lambda_+-K_1^{\mathrm{I}}-W=K_1^{\mathrm{II}}+(W/p)-\lambda_-$. In Eq. (10), E_1^{I}, E_2^{II}, C_+, and C_- are integral constants determined by the initial conditions.

Now a microwave recovery experiment is considered. In this experiment a short-microwave pulse resonant with the $T_1^{\mathrm{I}}\rightarrow T_2^{\mathrm{I}}$ and $T_1^{\mathrm{II}}\rightarrow T_2^{\mathrm{II}}$ transitions is applied at $t=0$ under continuous optical excitation, and the emission intensity of the N-V centers is monitored as a function of time. Two of the initial conditions are $N_*^{\mathrm{I}}(0)=N_*^{\mathrm{I}}(\infty)$ and $N_*^{\mathrm{II}}(0)=N_*^{\mathrm{II}}(\infty)$, which lead to

$$E_1^{\mathrm{I}}=E_+^{\mathrm{I}}+E_-^{\mathrm{I}},\quad E_2^{\mathrm{II}}=E_+^{\mathrm{II}}+E_-^{\mathrm{II}} . \tag{11}$$

Since the emissions from the subensembles I and II are detected at the same time, the observed transient is a superposition of four exponentials:

$$I(t)-I(\infty)=E_1e^{-\lambda_1 t}+E_2e^{-\lambda_2 t}-E_+e^{-\lambda_+ t}-E_-e^{-\lambda_- t} . \tag{12}$$

From Eq. (11), a relation

$$E_1+E_2=E_++E_-$$

holds since the emission intensity $I(t)$ is a linear combination of $N_*^{\mathrm{I}}(t)$ and $N_*^{\mathrm{II}}(t)$.

As is seen in Eq. (9), the decay constants λ_+ and λ_- are determined by the CR rate W as well as by the optical excitation rates K_1^{I} and K_1^{II}. In the limiting case of zero-excitation laser power, i.e., $K_1^{\mathrm{I}}=K_1^{\mathrm{II}}=0$, λ_+ and λ_- become $(1+1/p)W$ and 0, respectively. Therefore, if we can measure the value of λ_+ in the limit of zero laser power, it enables us to determine the CR rate W.

Now we examine the ratio E_+/E_- of the two amplitudes of the exponentials with decay constants λ_+ and λ_- in Eq. (12). For this purpose another initial condition is introduced:

$$\frac{N_1^{\mathrm{I}}(0)-N_1^{\mathrm{I}}(\infty)}{N_1^{\mathrm{II}}(0)-N_1^{\mathrm{II}}(\infty)}=\frac{N_1^{\mathrm{I}}(\infty)-N_2^{\mathrm{I}}(\infty)}{N_1^{\mathrm{II}}(\infty)-N_2^{\mathrm{II}}(\infty)} ,$$

which states that the population change induced by the microwave pulse is proportional to the population difference of the triplet sublevels before the pulse. Since $N_1^{\mathrm{I}}(0)$ and $N_1^{\mathrm{II}}(0)$ contain the integral constants C_+ and C_-, which appeared in Eq. (10), this condition determines the relation between C_+ and C_-. Explicit expressions for $N_1^{\mathrm{I}}(0)$, $N_1^{\mathrm{I}}(\infty)$, $N_2^{\mathrm{I}}(\infty)$, $N_1^{\mathrm{II}}(0)$, $N_1^{\mathrm{II}}(\infty)$, and $N_2^{\mathrm{II}}(\infty)$ are

$$N_1^{\mathrm{I}}(0)=N_1^{\mathrm{I}}(\infty)-\frac{(W/p)C_++QC_-}{(Q^2+W^2/p)(1+\alpha)} ,$$

$$N_1^{\mathrm{I}}(\infty)=\frac{\alpha}{1+\alpha}N^{\mathrm{I}}+\frac{(W/p)B_++QB_-}{2(Q^2+W^2/p)(1+\alpha)} ,$$

$$N_2^{\mathrm{I}}(\infty)=N^{\mathrm{I}}-N_1^{\mathrm{I}}(\infty) ,$$

$$N_1^{\mathrm{II}}(0)=N_1^{\mathrm{II}}(\infty)+\frac{QC_+-WC_-}{(Q^2+W^2/p)(1+\alpha)} ,$$

$$N_1^{\mathrm{II}}(\infty)=\frac{\alpha}{1+\alpha}N^{\mathrm{II}}+\frac{-QB_++WB_-}{2(Q^2+W^2/p)(1+\alpha)} ,$$

$$N_2^{\mathrm{II}}(\infty)=N^{\mathrm{II}}-N_1^{\mathrm{II}}(\infty) ,$$

where

$$B_+=\frac{2\alpha}{\lambda_+}(-K_2^{\mathrm{I}}WN^{\mathrm{I}}+K_2^{\mathrm{II}}QN^{\mathrm{II}}) ,$$

$$B_-=-\frac{2\alpha}{\lambda_-}(K_2^{\mathrm{I}}QN^{\mathrm{I}}+K_2^{\mathrm{II}}(W/p)N^{\mathrm{II}}) .$$

Using these expressions, we obtain

$$\frac{C_+}{C_-}=\frac{(\alpha-1)(WN^{\mathrm{I}}-QN^{\mathrm{II}})+B_+}{(\alpha-1)(Q+W)N^{\mathrm{I}}+B_-} . \tag{13}$$

In the limiting case of zero laser power, we obtain

$$\frac{E_+^{\mathrm{I}}}{E_-^{\mathrm{I}}}=\frac{W/p}{Q}\frac{C_+}{C_-}\rightarrow 0 ,$$

$$\frac{E_+^{\mathrm{II}}}{E_-^{\mathrm{II}}}=-\frac{Q}{W}\frac{C_+}{C_-}\rightarrow 0 ,$$

and thus

$$\frac{E_+}{E_-}\rightarrow 0\quad\text{or}\quad\frac{E_+}{E_++E_-}\rightarrow 0 . \tag{14}$$

This states that when the excitation laser power is very low, so that $W\gg K_1^{\mathrm{I}}$ and K_1^{II}, the amplitude E_+ of the component $\exp(-\lambda_+ t)$ becomes small compared with the amplitude E_- of the component $\exp(-\lambda_- t)$ and, in the limiting case of zero laser power, becomes zero. This is shown schematically in Fig. 3(a). Before the microwave pulse, the spin temperatures of subensembles I and II are equal because of the fact that the CR rate is much larger than the optical excitation rate $(a-1)$. After application of a π microwave pulse, the sublevel populations of each subensemble are inverted, but still have identical spin temperatures $(a-2)$, and therefore a net energy transfer with a rate of $\lambda_+\cong(1+1/p)W$ does not occur. Finally, the sublevel populations relax into the stationary state $(a-3)$ with a rate λ_-, which is determined only by the optical excitation rates.

In summary, in zero magnetic field, the emission intensity of the N-V center shows a time dependence according to Eq. (12) after an initial microwave pulse at $t=0$ has been applied. The transient is a superposition of four exponentials with rate constants λ_1, λ_2, λ_+, and λ_-,

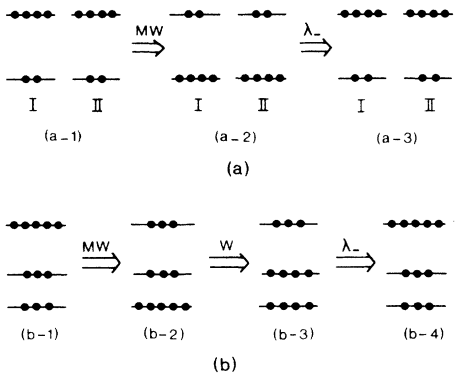

FIG. 3. Schematic picture of the time dependence of the spin alignment in the N-V center ground triplet sublevels in the microwave recovery experiments when the CR rate is much faster than the optical excitation rates. (a) $H=0$ G and (b) $H=514$ G. Detailed explanation of the figure is given in the text.

which are defined in Eq. (9). In the limiting case of zero-excitation laser power, λ_+ becomes $(1+1/p)W$ and λ_- becomes zero, and the ratio of the amplitudes E_+ and E_- of the exponentials $\exp(-\lambda_+ t)$ and $\exp(-\lambda_- t)$ becomes zero [Eq. (14)].

B. CR with a doublet spin system in the presence of a magnetic field

We consider CR between the diamond N-V center and a doublet spin species in the presence of an externally applied magnetic field. Upon application of a magnetic field, the doublet degeneracy of the triplet sublevels of the N-V center is lifted. Therefore a model consisting of four energy levels of subensemble I of the N-V center, the ground-state triplet sublevels T_α, T_β, and T_γ, and the excited state T_* is considered. CR occurs when the energy difference between the triplet sublevels T_β and T_γ equals the energy difference between the two spin states of a doublet species.[3] Using Eq. (2), the time dependence of the T_β-level population due to CR under relatively low excitation laser power is described by the rate equation

$$\frac{dN_\beta}{dt}=-\frac{W}{2}\left\{(N_\beta-N_\gamma)-\frac{N}{M}(M_1-M_2)\right\}, \tag{15}$$

where N_β and N_γ represent the populations of the T_β and T_γ triplet sublevels and M_1 and M_2 represent the populations of the doublet spin states as shown in Fig. 2(b); N and M are the total number of spins of subensemble I of the N-V center and of the $g=2.00$ doublet species, respectively. We assume that the doublet species form a spin reservoir with a much larger heat capacity than the triplet subensemble considered. Furthermore, it is assumed that there is a fast energy transfer within the reservoir so that the doublet species is always kept at a constant spin temperature identical to the lattice temperature T. With the present lattice temperature at 1.4 K, $(N/M)(M_1-M_2)$ is approximately zero.

The rate equations for the populations of the four energy levels of the N-V center subensemble become

$$\begin{aligned}
\frac{dN_*}{dt}&=k_\alpha N_\alpha+k_\beta N_\beta+k_\gamma N_\gamma-(A_\alpha+A_\beta+A_\gamma)N_*\ ,\\
\frac{dN_\alpha}{dt}&=-k_\alpha N_\alpha+A_\alpha N_*\ ,\\
\frac{dN_\beta}{dt}&=-k_\beta N_\beta+A_\beta N_*-\frac{W}{2}(N_\beta-N_\gamma)\ ,\\
\frac{dN_\gamma}{dt}&=-k_\gamma N_\gamma+A_\gamma N_*+\frac{W}{2}(N_\beta-N_\gamma)\ ,
\end{aligned} \tag{16}$$

where k_i and A_i $(i=\alpha,\beta,\gamma)$ are the optical excitation rate of the sublevel T_1 and the decay rate constant from the excited level T_* into the ground sublevel T_1, respectively. An additional condition

$$N_\alpha+N_\beta+N_\gamma+N_*=N \tag{17}$$

reduces the number of independent variables to 3.

Assuming for simplicity that

$$A_\alpha=A_\beta=\xi A_\gamma\ , \tag{18}$$

Eq. (16) is solved analytically. N_*, $P_1=N_\alpha-\xi N_\gamma$, and $P_2=N_\beta-\xi N_\gamma$ are chosen as the three independent variables. Neglecting terms as $k_\alpha N_*$, which are small compared to, e.g., $k_\alpha N_\alpha$, the rate equations for the three variables become

$$\frac{d}{dt}\bar{a}=\bar{A}-R\bar{a}\ , \tag{19}$$

where

$$\bar{A}=\begin{pmatrix}\left[\dfrac{k_\gamma}{1+2\xi}-S_1-S_2\right]N\\ \left\{S_1+\dfrac{(1-\xi)\xi}{1+2\xi}\dfrac{W}{2}\right\}N\\ \left\{S_2+\dfrac{1-\xi^2}{1+2\xi}\dfrac{W}{2}\right\}N\end{pmatrix},\quad \bar{a}=\begin{pmatrix}N_*\\P_1\\P_2\end{pmatrix},$$

$$R=\begin{pmatrix}A_1+A_2+A_3 & -F_1 & -F_2\\ 0 & T_1+\dfrac{(1-\xi)\xi}{1+2\xi}\dfrac{W}{2} & S_1+\dfrac{(2+\xi)\xi}{1+2\xi}\dfrac{W}{2}\\ 0 & S_2+\dfrac{1-\xi^2}{1+2\xi}\dfrac{W}{2} & T_2+\dfrac{(\xi+1)(\xi+2)}{1+2\xi}\dfrac{W}{2}\end{pmatrix},$$

$$S_1=\frac{\xi(k_\gamma-k_\alpha)}{1+2\xi},\quad S_2=\frac{\xi(k_\gamma-k_\beta)}{1+2\xi},$$
$$T_1=\frac{(1+\xi)k_\alpha+\xi k_\gamma}{1+2\xi},\quad T_2=\frac{(1+\xi)k_\beta+\xi k_\gamma}{1+2\xi},$$
$$F_1=\frac{(1+\xi)k_\alpha-\xi k_\beta-k_\gamma}{1+2\xi},\quad F_2=\frac{-\xi k_\alpha+(1+\xi)k_\beta-k_\gamma}{1+2\xi}.$$

The three eigenvalues of the matrix R are

$$\lambda_1=A_1+A_2+A_3,$$
$$\lambda_\pm=\tfrac{1}{2}\left[T_1+T_2+W\pm\left[(T_1+T_2+W)^2-4\left\{T_1+\frac{\xi(1-\xi)}{1+2\xi}\frac{W}{2}\right\}\left\{T_2+\frac{(\xi+1)(\xi+2)}{1+2\xi}\frac{W}{2}\right\}+4\left\{S_1+\frac{\xi(2+\xi)}{1+2\xi}\frac{W}{2}\right\}\left\{S_2+\frac{1-\xi^2}{1+2\xi}\frac{W}{2}\right\}\right]^{1/2}\right]. \tag{20}$$

After application of a microwave pulse resonant with the $T_\gamma\rightarrow T_\alpha$ transition at $t=0$, the time dependence of N_* becomes

$$N_*(t)-N_*(\infty)=(E_++E_-)e^{-\lambda_1 t}-E_+e^{-\lambda_+ t}-E_-e^{-\lambda_- t}. \tag{21}$$

The amplitudes of the two exponential components $\exp(-\lambda_+ t)$ and $\exp(-\lambda_- t)$ become

$$E_+=\frac{1}{D\lambda_1}\left[F_1R+F_2\left\{S_2+\frac{1-\xi^2}{1+2\xi}\frac{W}{2}\right\}\right]C_+,$$
$$E_-=\frac{1}{D\lambda_1}\left[-F_1\left\{S_1+\frac{\xi(2+\xi)}{1+2\xi}\frac{W}{2}\right\}+F_2R\right]C_-, \tag{22}$$

where,

$$R=T_1+\frac{\xi(1-\xi)}{1+2\xi}\frac{W}{2}-\lambda_-=\lambda_+-T_2-\frac{(\xi+1)(\xi+2)}{1+2\xi}\frac{W}{2},$$
$$D=R^2+\left\{S_1+\frac{\xi(2+\xi)}{1+2\xi}\frac{W}{2}\right\}\left\{S_2+\frac{1-\xi^2}{1+2\xi}\frac{W}{2}\right\},$$

and C_+ and C_- are integral constants determined by the initial conditions. In a similar manner as in Sec. II A, the ratio E_+/E_- is calculated using the initial condition $N_\beta(0)=N_\beta(\infty)$. We only show the results when the CR rate is much larger than the optical excitation rates, i.e., $W\gg k_1$ $(i=\alpha,\beta,\gamma)$:

$$\frac{E_+}{E_-}=\frac{-k_2+k_3}{-2k_1+k_2+k_3}, \tag{23}$$

which generally takes a finite value, in contrast to the zero-field case described in Sec. II A.

A qualitative explanation of the finite amplitude E_+ in the case of $W\gg k_i$ is presented in Fig. 3(b). Before the microwave pulse is applied, N_β and N_γ are nearly equal because of the fast CR with the doublet species $(b-1)$. After application of a π microwave pulse, the populations N_α and N_γ are inverted $(b-2)$, destroying the equilibrium between N-V center spins and the doublet spins. As a result, a net energy transfer with the rate $\lambda_+\cong W$ takes place, redistributing the populations N_β and N_γ $(b-3)$. Then a slow relaxation takes place into the final stationary state $(b-4)$ with a rate λ_- which is determined by the optical excitation rates.

In the experiments discussed in Sec. IV, λ_+ and λ_- are measured as a function of the external magnetic-field strength under a fixed, relatively low, excitation laser power, with which the excitation rates become of the same order of magnitude as the CR rate W. Since Eq. (20) includes too many parameters, it is not possible to obtain the exact value of W from experimental results. However, λ_+ and λ_- in Eq. (20) are approximated by the expressions

$$\lambda_+=K_++W \quad\text{and}\quad \lambda_-=K_-, \tag{24}$$

where K_+ and K_- represent the rates λ_+ and λ_- when $W=0$, respectively. This is verified from a numerical analysis which shows that the approximation in Eq. (24) leads to a less than a few percent error in the determination of W when $T_2/T_1\geq 1$ and $\xi\leq 1$. For example, when $T_2/T_1=2$, $S_1/T_1=0.2$, $S_2/T_1=0.4$, $\xi=0.5$, and $W/T_1=5$, λ_+/T_1 and λ_-/T_1 are calculated to be 7.10 and 0.905, respectively, from Eq. (20). On the other hand, when λ_+/T_1 and λ_-/T_1 are calculated using the approximation of Eq. (24), the values are $\lambda_+/T_1=7.07$ and $\lambda_-/T_1=0.926$, in good agreement with the exact results. In Sec. IV we will see that the approximation of Eq. (24) is satisfactory also for our experimental results.

Thus far, we have analyzed the kinetics with a finite CR rate W. Now we deal with a special case when $W=0$, which will become useful in Sec. IV. In this case the time dependence of the emission intensity after a microwave pulse at $t=0$ becomes a superposition of three exponential curves [Eq. (21)] with rate constants:

$$\lambda_1 = A_1 + A_2 + A_3 ,$$
$$\lambda_\pm = \frac{1}{2(1+2\xi)}\{(1+\xi)(k_\alpha + k_\beta) + 2\xi k_\gamma \pm [(1+2\xi-\xi^2)(k_\alpha - k_\beta)^2 + 2\xi^2(k_\beta - k_\gamma)^2 + 2\xi^2(k_\alpha - k_\gamma)^2]^{1/2}\} . \quad (25)$$

This result can be applied to subensemble II as well as to subensemble I. It is important to mention that, when the two excitation rates k_α and k_β are the same, either E_+ or E_- in Eq. (21) becomes zero depending on whether $k_\gamma < k_\alpha = k_\beta$ or $k_\gamma > k_\alpha = k_\beta$, respectively. Thus, in this case, the microwave recovery transient becomes a sum of two exponentials $\exp(-\lambda_1 t)$ and $\exp(-\lambda_+ t)$ [or $\exp(-\lambda_- t)$]. This result is easily understood since, as long as our interest is in the time dependence of N_*, the system becomes a three-level system ($T_\alpha + T_\beta$), T_γ, and T_*) instead of the four-level system (T_α, T_β, T_γ, and T_*) when $k_\alpha = k_\beta$ and $W = 0$, and a three-level system with homogeneous rate equations generally has a biexponential solution.

In summary, when CR occurs between a subensemble of N-V center spins and a doublet spin species in the presence of an external magnetic field, the microwave recovery transient is given by Eq. (21) with rate constants given by Eq. (20). Equation (20) is well approximated by Eq. (24). When no CR occurs in a magnetic field, the microwave recovery transient also has the form Eq. (21), but now with decay constants expressed by Eq. (25). When $k_\alpha = k_\beta$ and $W = 0$, one of the amplitudes E_+ and E_- in Eq. (21) becomes zero, and the recovery transient becomes a biexponential function with two decay constants λ_1 and λ_+ (or λ_-).

III. EXPERIMENTAL DETAILS

The brown-colored diamond crystal investigated here was the same as used previously (crystal A).[11,15] Occasionally, another diamond crystal (crystal B) (Refs. 3, 4, and 8) was used in which the N-V center concentration is less by about a factor 5 than in crystal A. Most of the results described in Sec. IV are for crystal A unless mentioned otherwise. The crystal was mounted inside a slow-wave helix immersed in a pumped liquid-helium bath ($T = 1.4$ K). Optical excitation was at 514 nm using a cw Ar^+-ion laser (Spectra Physics series 2000). The fluorescence emitted perpendicular to the exciting light was focused on the entrance slit of a monochromator. Photodetection was at 637 nm using a GaAs photomultiplier tube HAMAMATSU R943-02. The spectrometer used in the optically detected magnetic resonance (ODMR) experiments has been described elsewhere.[16] The time-resolved microwave recovery of the emission intensity[11,15] was measured after a microwave pulse of a duration of typically 0.2 μs was applied under continuous optical excitation. The microwave-pulse intensity corresponded to a Rabi frequency of approximately 3 MHz. The transient signal was accumulated on a PAR model 4202 signal average.

IV. RESULTS

A. Polarization dependence of the optical excitation rate of the N-V center

When an external magnetic field is applied along the [111] axis of the diamond crystal, the ensemble of N-V centers is divided into two subensembles I and II.[3] Subensemble I consists of the N-V centers whose molecular main axes are oriented along the magnetic field. Subensemble II, on the other hand, consists of N-V centers whose molecular main axes are oriented along either the $[1\bar{1}\bar{1}]$, $[\bar{1}1\bar{1}]$, or $[\bar{1}\bar{1}1]$ direction (cf. Fig. 1). A microwave recovery experiment was performed for subensemble I in the presence of an external magnetic field of 30 G applied along the [111] axis. In this experiment the time dependence of the emission intensity of the N-V center is monitored after the application of a microwave pulse under continuous optical excitation. By adjusting the microwave frequency to the $T_\gamma \rightarrow T_\alpha$ resonance frequency of subensemble I, the microwave recovery transient due to the intensity change of the subensemble-I emission can be obtained. Figure 4 shows the microwave recovery transients for subensemble I when the polarization direction of the laser light is parallel (curve a) or perpendicular (curve b) to the molecular main axis. The recovery transient has a very fast rise at $t = 0$ with a time constant shorter than the time resolution of the present experiment (< 10 μs) and has a subsequent slower

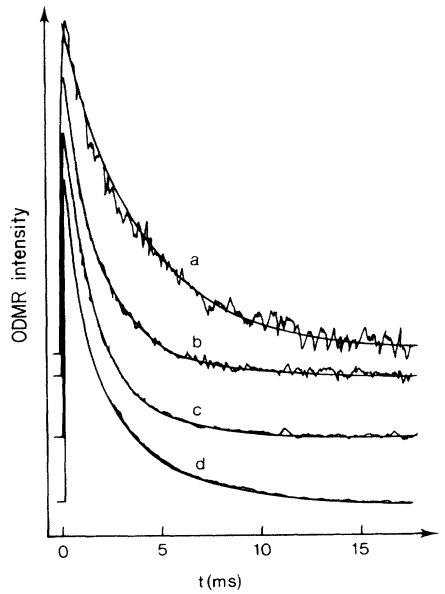

FIG. 4. Optically detected microwave recovery transients of N-V center in diamond. Excitation laser power, 0.5 W at 514 nm; detection wavelength, 637 nm; and $T = 1.4$ K. Subensemble I, $H = 30$ G (curve a) (excitation light polarization) $\parallel$ (molecular main axis); subensemble I, $H = 30$ G (curve b) (light polarization) $\perp$ (molecular main axis); subensemble II; $H = 30$ G (curve c) (light polarization) $\parallel$ [111]; and subensembles I and II, $H = 0$ G (curve d) (light polarization) $\parallel$ [111]. $\mathbf{H} \parallel [111]$. The drawn curves are the best fits to a monoexponential function (curve a) and to a biexponential function (curves b–d).

recovery. The kinetic analysis in Sec. II B indicates that the initial fast rise is determined solely by the decay rates of the optically excited N-V center to the ground-state triplet sublevels and that the subsequent slower recovery is determined by the optical excitation rates of the triplet sublevels in the absence of CR. Since the initial fast rise is faster than the time resolution of the present experiment, only the subsequent slower recovery is examined in this paper. Comparing the two microwave recovery transients a and b in Fig. 4, it is found that the recovery rate is larger when the excitation light is polarized perpendicular to the molecular main axis. This shows that the optical excitation rates of the N-V center strongly depend on the polarization direction of the excitation light. As has been shown in Sec. II B, the recovery transient generally has a biexponential form if we neglect the initial fast rise with decay constant λ_1 in Eq. (21). When the excitation light is polarized along the molecular main axis, however, the microwave recovery transient closely resembles a monoexponential curve, which indicates that the optical excitation rates k_α and k_β of two triplet sublevels become equal, as was shown in Sec. II B. Curve a in Fig. 4 has been fitted by a monoexponential curve with a decay rate constant of 2.5×10^2 s^{-1}. Curve b in Fig. 4, on the other hand, deviates from a monoexponential decay, indicating that $k_\alpha \neq k_\beta$, and has been fitted to a biexponential curve with decay rate constants of 1.8×10^3 and 4.6×10^2 s^{-1}. Thus the excitation rate constant becomes several times faster when the excitation light is polarized perpendicular to the molecular main axis. The deviation from the monoexponential recovery, i.e., $k_\alpha \neq k_\beta$, of curve b may be due to the fact that the light polarization direction is not along the symmetry axis of the N-V center, although the physical meaning is unknown at present.

A microwave recovery transient for subensemble II with the same excitation laser power as in the above two cases is shown by curve c of Fig. 4. This transient has been obtained by application of a microwave pulse resonant with the $T_\gamma \rightarrow T_\alpha$ ODMR transition of subensemble II, in the presence of a magnetic field of 30 G along the [111] direction. The polarization direction of the excitation light is along the [111] axis, so that the N-V centers belonging to subensemble II have their molecular main axes tilted by 109° 28′ from the polarization direction. As is illustrated in Fig. 4, the microwave recovery is faster for subensemble II than for subensemble I, for which the polarization direction is parallel to the [111] axis. This agrees with the polarization dependence of the excitation rate already noted for subensemble I. Thus subensembles I and II have different excitation rates when the polarization direction of the excitation light is along the [111] axis. As a result, the spin temperatures of the two subensembles become different upon cw optical excitation.

B. CR effect on optically detected microwave recovery transients at zero magnetic field

In zero magnetic field, N-V center subensembles I and II become magnetically equivalent; i.e., the energy separations of the ground-state triplet sublevels become equal. The spin temperatures of the two subensembles, however, will be different when continuous optical excitation with the polarization direction along the [111] axis is applied, as has been discussed in Sec. IV A. As a result, CR takes place between the two subensembles I and II. The effects of CR on the fluorescence intensity and spin dephasing rate have been studied in a previous paper.[3] Here we study the effect on the microwave recovery rate, which directly reflects the energy-transfer rate due to CR.

The microwave recovery at zero magnetic field was measured using microwave pulses resonant with both subensembles I and II, at a frequency of 2880 MHz. A typical recovery transient is shown in Fig. 4 (curve d), which is fitted by a biexponential function

$$I(t)-I(\infty)=-E_+e^{-\lambda_+ t}-E_-e^{-\lambda_- t}. \tag{26}$$

The experiment was performed for a series of laser excitation powers, and the obtained rates λ_+ and λ_- are plotted in Fig. 5(a) as a function of the laser power. The microwave recovery rates strongly depend on the laser power because they reflect the population relaxation rates of the ground-state triplet sublevels, and therefore the recovery rates increase with increasing laser power. When the values of λ_+ and λ_- are extrapolated to zero

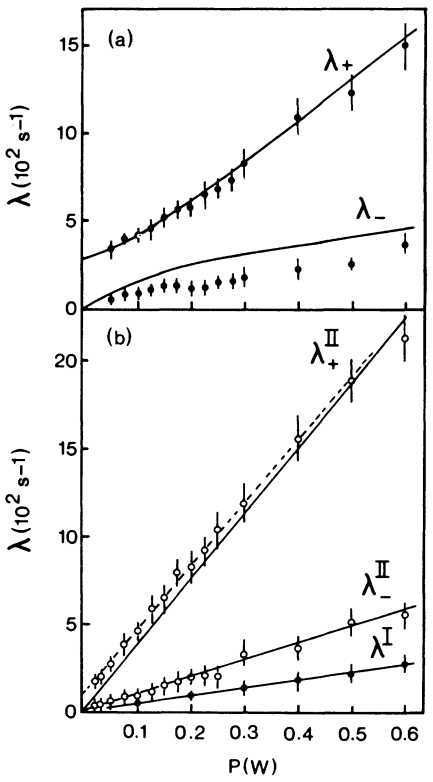

FIG. 5. Excitation laser power dependence of the decay rate constants of biexponential ($\lambda_+,\lambda_-,\lambda_+^{II},\lambda_-^{II}$) and monoexponential ($\lambda^I$) microwave recovery transients. (Excitation light polarization) $\|[111]$. (a) $H=0$ G and (b) $H=30$ G along [111]. The solid lines are the calculated ones using Eqs. (9) and (25) with parameter values given in the text. The dashed line for λ_+^{II} is the best fit of the data points to a linear function.

laser power, λ_+ takes a finite value of $(2.7\times0.4)\times10^2$ s^{-1} whereas λ_- becomes zero. The residual recovery rate of λ_+ at zero laser power indicates the existence of a population relaxation process which is not induced by optical excitation. As will be shown in Sec. IV C, the residual value of λ_+ at the zero laser power is substantially reduced in the presence of a magnetic field of 30 G. In this case subensembles I and II are no longer magnetically equivalent, and CR cannot take place between them. Thus the presence of a nonzero value for λ_+ in the case of zero magnetic field shows that in zero field CR dynamics between the two subensembles is probed.

In Sec. II A the CR effect on the microwave recovery transient at zero magnetic field has been analyzed using a triplet-state kinetic scheme. The analysis of Sec. II A shows that the values of λ_+ and λ_- become $(1+1/p)W$ and 0, respectively, in the case of vanishing optical excitation rates. Here W denotes the CR rate of the triplet spins in subensemble I [cf. (Eq. (3)], and p is the ratio of the spin numbers belonging to subensembles II and I, which takes a value 3 in the present case. The expected behaviors of λ_+ and λ_- in the limiting case of the zero excitation rates are exactly as observed in the microwave recovery experiments and are shown in Fig. 5(a). From the residual value of λ_+ at the zero laser power, the CR rate is estimated to be $(2.0\pm0.3)\times10^2$ s^{-1}. The kinetic analysis presented in Sec. II A also shows that the ratio E_+/E_- of the amplitudes of the two exponential components in Eq. (26) becomes zero in the limiting case of zero laser power [cf. Eq. (14)]. This is in fact observed in the present experiment, as is shown in Fig. 6(a). In Fig. 6(a) it can be seen that the ratio $E_+/(E_++E_-)$ decreases steeply as the laser power decreases below 0.2 W.

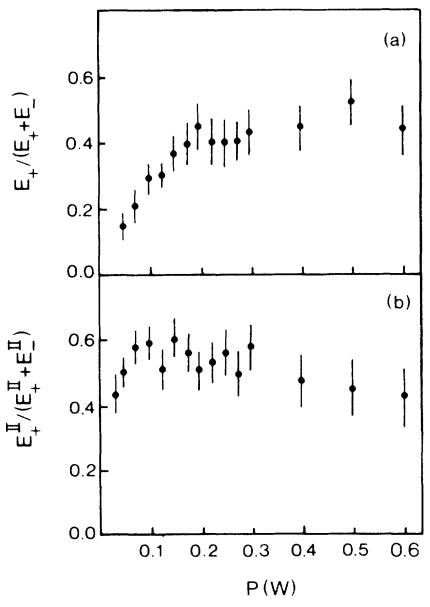

FIG. 6. Excitation laser power dependence of the ratio of the amplitudes E_+ and E_- of the two exponential components of a biexponential microwave recovery. (a) $H=0$ G and (b) $H=30$ G along [111].

Thus the experimental results in the limit of the zero laser power are satisfactorily explained on the basis of a CR process between the two subensembles I and II, and a CR rate of $(2.0\pm0.3)\times10^2$ s^{-1} is estimated. A more detailed comparison between the experimental results and the kinetic analysis in Sec. II will be given in Sec. IV D.

It is noted that the residual value of λ_+ in the limit of zero laser power in Fig. 5(a) cannot be attributed to spin-lattice relaxation. In the event of spin-lattice relaxation, λ_- must have the same residual value as λ_+, and $E_+/(E_++E_-)$ does not become zero. This is seen directly as follows. The N-V center in each subensemble consists of three energy levels at zero magnetic field, i.e., two sublevels of the axially symmetric ground triplet state and an excited state. Because of the restriction that the total spin number be constant, there are two independent variables, e.g., N_1^I and N_2^I in Sec. II A. Thus the microwave recovery transient of each subensemble becomes a superposition of two exponential curves:

$$F_1e^{-\lambda_1t}+F_2e^{-\lambda_2t}\quad(\lambda_1\gg\lambda_2)\ .$$

The recovery rate λ_1 is solely determined by the decay rates of the excited state of the N-V center, while λ_2 is determined by the optical excitation rate and spin-lattice relaxation rate. The first term $F_1\exp(-\lambda_1t)$ can be neglected since it decays much faster than the time resolution of the experiment presently considered. Thus the observed microwave recovery transient of each subensemble becomes a monoexponential curve, and in the present experimental results, the exponential components with the rate constants of λ_+ and λ_- are attributed to subensembles II and I, respectively. Since the two subensembles must have almost the same spin-lattice relaxation rate, λ_+ and λ_- must have almost the same residual value in the limit of zero laser power. Furthermore, the amplitude E_+ of the $\exp(-\lambda_+t)$ component must always have a larger value than the amplitude E_- of the $\exp(-\lambda_-t)$ component because subensemble II has a 3 times larger spin number and a much larger optical excitation rate and, as a result, a larger contribution to the emission intensity than subensemble I. It is therefore concluded that the observed residual value of λ_+ with the zero laser power in Fig. 5(a) is not due to spin-lattice relaxation and that spin-lattice relaxation is a much slower process at the lattice temperature of 1.4 K.

The CR rate at zero magnetic field has also been measured for the diamond crystal B.[3,4,8] From a comparison of the HED rate constants of the N-V centers in samples A and B, we find that crystal B contains a 5 times lower concentration of N-V centers than crystal A. Crude estimates based on EPR intensity measurements are in agreement with this concentration ratio. From the extrapolated value of $(0.7\pm0.3)\times10^2$ s^{-1} for λ_+ as the laser power goes to zero, the CR rate is estimated to be $(0.5\pm0.2)\times10^2$ s^{-1} for crystal B, which is about 4 times slower than the CR rate for crystal A, in agreement with the N-V center concentration ratio. An equivalent experimental result for crystal B has already been reported[17] using adiabatic fast-passage experiments instead of microwave recovery techniques. In the adiabatic fast-

passage experiment,[17] the extrapolated value of λ_+ to zero laser power is about 0.7×10^2 s^{-1}, in agreement with the present result, although the meaning of this finite extrapolated value of λ_+ was not discussed in Ref. 17.

C. N-V center kinetics in the absence of CR

In a magnetic field of 30 G along the [111] axis, subensembles I and II are no longer resonant, and therefore CR does not take place between them. In the presence of this magnetic field, the microwave recovery transient was observed with the polarization of the excitation light along the [111] axis. Typical recovery transients were already shown in Fig. 4 when the microwaves are resonant with the $T_\gamma\rightarrow T_\alpha$ ODMR transition at frequencies of 2.95 and 2.89 GHz of subensembles I and II, respectively. For subensemble I the microwave recovery transients are fitted to a monoexponential function with a rate constant $\lambda^{\rm I}$, and the obtained value for $\lambda^{\rm I}$ is plotted in Fig. 5(b) as a function of the excitation laser power. $\lambda^{\rm I}$ shows a linear dependence on the laser power and is extrapolated to zero when the laser power goes to zero. This is as expected because in a magnetic field of 30 G subensemble I does not take part in any CR process with subensemble II or with $g=2$ doublet spin species. For subensemble II the microwave recovery transient is fitted to a biexponential function with rate constants $\lambda_+^{\rm II}$ and $\lambda_-^{\rm II}$. The values of $\lambda_+^{\rm II}$ and $\lambda_-^{\rm II}$ are plotted in Fig. 5(b). Both $\lambda_+^{\rm II}$ and $\lambda_-^{\rm II}$ show linear dependences on the laser power. From Fig. 5(b) it can be seen that when the laser power goes to zero $\lambda_+^{\rm II}$ is extrapolated to $(1.0\pm0.3)\times10^2$ s^{-1}, which indicates the existence of a residual population relaxation process other than optical excitation. This extrapolated value of $\lambda_+^{\rm II}$, however, is significantly smaller than that at zero magnetic field, at which it is $(2.7\pm0.4)\times10^2$ s^{-1}. The difference between the extrapolated values at 0 and 30 G is certainly due to the fact that in zero field CR occurs between subensembles I and II.

The ratio $E_+^{\rm II}/(E_+^{\rm II}+E_-^{\rm II})$ of the amplitudes of the two exponential components of the microwave recovery transient for subensemble II is plotted in Fig. 6(b). It is seen in Fig. 6(b) that this ratio does not exhibit any significant decrease at low laser power in contrast to the result shown in Fig. 6(a). This result is also in agreement with the conclusion of Sec. IV B, that the residual population relaxation observed at zero magnetic field is due to CR between subensembles I and II.

The residual population relaxation rate for subensemble II in a magnetic field of 30 G is approximately 1×10^2 s^{-1}, as determined from the extrapolated value of $\lambda_+^{\rm II}$ to zero laser power in Fig. 5(b). This relaxation process may be due to CR inside subensemble II. If all the N-V centers belonging to subensemble II have identical optical excitation rates, the flip-flop (or CR) processes inside subensemble II would not be detected by a microwave recovery experiment because such flip-flop processes do not change the emission intensity. However, if there is a distribution in the optical excitation rates of the N-V centers in subensemble II, the energy transfer by the flip-flops inside subensemble II causes a change in the emission intensity and can, in principle, be detected. The following possibilities for the origin of the disparity in the optical excitation may be mentioned. (i) There is a small misalignment of the polarization direction from the [111] axis so that the three different sites belonging to subensemble II shown in Fig. 1 are not optically equivalent. (ii) There is an intrinsic inhomogeneity in the optical excitation rate of N-V centers. (iii) The excitation light intensity is inhomogeneous in the crystal. In any case a detailed analysis of the triplet-state kinetics becomes much too complicated and is beyond the scope of this paper.

D. Influence of the laser power on N-V center spin kinetics

In this subsection the laser power dependences of the experimentally obtained rate constants shown in Fig. 5 are considered on the basis of Eqs. (9) and (25). At zero magnetic field, the rate constants of the biexponential microwave recovery are expressed by Eq. (9), which contains three parameters $K_1^{\rm I}=(k_1^{\rm I}+\alpha k_2^{\rm I})/(1+\alpha)$, $K_1^{\rm II}=(k_1^{\rm II}+\alpha k_2^{\rm II})/(1+\alpha)$, and W. With the magnetic field of 30 G, the rate constants $\lambda_+^{\rm II}$ and $\lambda_-^{\rm II}$ for subensemble II are expressed by Eq. (25), which contains four parameters $k_\alpha^{\rm II}$, $k_\beta^{\rm II}$, $k_\gamma^{\rm II}$, and $\xi^{\rm II}$. For subensemble I, in a magnetic field of 30 G, a monoexponential microwave recovery is observed, which means $k_\alpha^{\rm I}=k_\beta^{\rm I}$, as has been discussed at the end of Sec. II B. In this case the monoexponential recovery rate becomes $\lambda^{\rm I}=(k_\alpha^{\rm I}+2\xi^{\rm I}k_\gamma^{\rm I})/(1+2\xi^{\rm I})$ from Eq. (25). Since the T_α and T_β sublevels in a field of 30 G become degenerate at zero magnetic field, it is a reasonable assumption that $k_1^{\rm I}=(k_\alpha^{\rm I}+k_\beta^{\rm I})/2=k_\alpha^{\rm I}$, $k_1^{\rm II}=(k_\alpha^{\rm II}+k_\beta^{\rm II})/2$, $k_2^{\rm I}=k_\gamma^{\rm I}$, $k_2^{\rm II}=k_\gamma^{\rm II}$, and $\alpha=2\xi^{\rm I}=2\xi^{\rm II}=2\xi$. Thus we have six parameters $K_1^{\rm I}$, $k_\alpha^{\rm II}$, $k_\beta^{\rm II}$, $k_\gamma^{\rm II}$, W, and ξ to explain all the recovery rates shown in Figs. 5(a) and 5(b). Since the optical excitation rates depend linearly on the laser power, the six parameters are rearranged as follows: $k_\alpha^{\rm II}/K_1^{\rm I}$, $k_\beta^{\rm II}/K_1^{\rm I}$, $k_\gamma^{\rm II}/K_1^{\rm I}$, $C=K_1^{\rm I}/P$, W, and ξ, where P represents the laser power in watts and C is the proportionality constant. The solid lines in Fig. 5 are calculated using the following values for the parameters: $k_\alpha^{\rm II}/K_1^{\rm I}=1.4$, $k_\beta^{\rm II}/K_1^{\rm I}=8.2$, $k_\gamma^{\rm II}/K_1^{\rm I}=9.6$, $C=4.5\times10^2$ s^{-1}W^{-1}, $W=2.0\times10^2$ s^{-1}, and $\xi=0.1$. As is seen in Fig. 5, Eqs. (9) and (25) on the whole can satisfactorily explain the experimental points, although the agreement is less for λ_- at zero magnetic field and for $\lambda_+^{\rm II}$ at a magnetic field of 30 G. It is concluded that the kinetic analysis presented in Sec. II A correctly predicts the special effects of CR on the microwave recovery kinetics near zero laser excitation power, whereas qualitative agreement is obtained for the results under conditions of finite laser power. One possible reason for the slight disparity with the experimental results in the latter case may be due to the distribution of the optical excitation rates within each subensemble, as discussed in Sec. IV C.

E. CR between N-V center and $g=2.00$ doublet species

In a magnetic field of 514 G applied along the [111] crystallographic axis, the N-V center subensemble I and a $g=2.00$ doublet species become resonant and CR takes place. A typical $g=2.00$ doublet species in diamond is

the P_1 center,[18–20] which consists of a single isolated nitrogen atom substitutional for a carbon atom. CR with the P_1 center is reflected as a sudden change in the emission intensity of the N-V center accompanied by hyperfine splittings originating from the P_1 centers. However, CR with the $g=2.00$ doublet species did not affect the spin-dephasing rate measured by spin-echo techniques. In this paper the effect of the CR with the $g=2$ doublet species is examined by the optically detected microwave recovery experiments. It must be noted, however, that the present study is for crystal A, whereas the results reported in Ref. 3 are for crystal B. In the two crystals, both the $g=2$ doublet species and the N-V centers may have different concentrations.

The microwave recovery experiment was performed using microwaves resonant with the $T_\gamma \rightarrow T_\alpha$ ODMR transition of subensemble I. The polarization direction of the cw optical excitation light was perpendicular to the molecular main axis of subensemble I, i.e., a $[0\bar{1}1]$ direction, because this polarization direction provides faster excitation rates and a stronger emission intensity for subensemble I. The microwave recovery transients obtained in this way are shown in Fig. 7 for magnetic-field strengths outside (curve a) and within (curve b) the CR region. From Fig. 7 it is clearly seen that the microwave recovery rate becomes substantially larger under CR conditions.

The experiment was performed for a series of magnetic-field strengths, using a constant laser excitation power. The microwave recovery transient is well fitted to a biexponential function [Eq. (26)] for all magnetic-field strengths, and the obtained rate constants λ_+ and λ_- are plotted in Fig. 8. It is seen in Fig. 8 that λ_+ is enhanced at the CR region, while λ_- takes an almost constant value. This result is well explained by the approximate formula Eq. (24), which was obtained from the kinetic

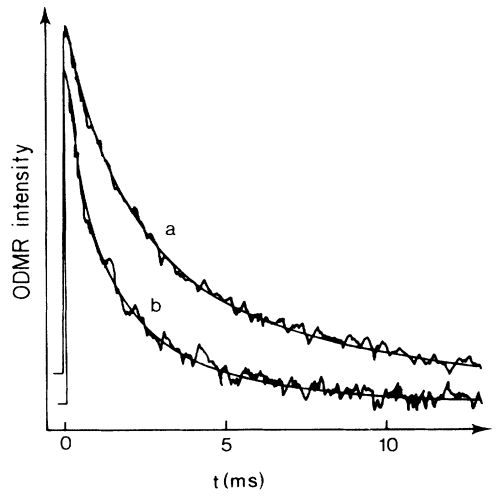

FIG. 7. Optically detected microwave recovery transients of the N-V center in subensemble I. Excitation laser power, 0.5 W; (laser polarization) $\perp$ [111]. $H=472$ G (curve a) (outside the CR region) and $H=514$ G (curve b) (center of the CR region). $\mathbf{H}\|[111]$. Drawn curves are best fits to a biexponential function.

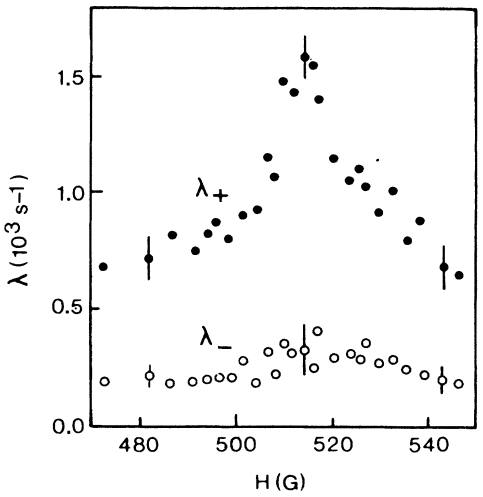

FIG. 8. Decay rate constants λ_+ and λ_- of the biexponential microwave recovery transients as a function of the external magnetic-field strength. $\mathbf{H}\|[111]$.

analysis in Sec. II B. Equation (24) states that the CR rate W is obtained from the difference of the λ_+ values inside and outside the CR region. Since the value of λ_+ is $(1.56\pm0.10)\times10^3$ s^{-1} at the center of the CR region and $(0.65\pm0.10)\times10^3$ s^{-1} outside the CR region, the CR rate is estimated to be $(9.1\pm1.4)\times10^2$ s^{-1}.

V. DISCUSSION

By means of microwave recovery experiments, a CR rate of $(2.0\pm0.3)\times10^2$ s^{-1} was estimated for the CR between the two subensembles I and II of N-V centers and a rate of $(9.1\pm1.4)\times10^2$ s^{-1} for the CR between subensemble I of N-V centers and a $g=2.00$ doublet species. These values are in quite good agreement with the CR rates estimated previously[11] for the 2.818-eV center excited triplet state in crystal A, namely, $(5.0\pm1.5)\times10^2$ s^{-1} for the CR between the 2.818-eV and N-V centers and $(8.0\pm2.5)\times10^2$ s^{-1} for the CR between the 2.818-eV center and $g=2.00$ doublet species. This agreement is reasonable because, if all spin species are randomly distributed in the crystal, N-V and 2.818-eV center spins experience, on the average, the same dipolar interaction from their surroundings.

In the following the present result is compared with the spin-echo results reported in Ref. 3. Since the results in Ref. 3 are for crystal B, the discussion should be restricted to the results for the same crystal. The CR rate obtained by the microwave recovery experiments for crystal B is 0.5×10^2 s^{-1} for the CR between the N-V center subensembles I and II. On the other hand, the Hahn echo decay (HED) rate is enhanced from 1.3×10^4 to 2.5×10^4 s^{-1}, the stimulated echo decay (SED) rate from 1.3×10^3 to 3.3×10^3 s^{-1}, and the spin-locking echo decay (SLD) rate from 2.4×10^2 to 5.3×10^2 s^{-1} as a result of CR between subensembles I and II.[3,4] Thus the time scale of the CR effect in the microwave recovery transients differs appreciably from that in the spin-echo

decays. A similar time-scale difference between the CR effects in the microwave recovery and spin-echo decay has been reported for the CR between F_2^{2+} and F^+ defects in CaO.[21] The origin of this difference is discussed in the following.

First, the origin of the optically detected microwave recovery is considered. The microwave recovery results from population relaxation processes after initial disturbance of the spin-level populations by a microwave pulse. Possible causes for this population relaxation are optical excitation, CR due to spin flip-flops, and spin-lattice relaxation. We restrict ourselves to a discussion of the spin flip-flops. Flip-flops only contribute to the microwave recovery rate when the spin species participating in the flip-flop process have different optical excitation and emission rates. Thus the spin flip-flops occurring between subensembles I and II are detected by the microwave recovery experiment only because the two subensembles have different optical excitation rates. Therefore spin flip-flops within subensemble I are not detectable because the participating spins have identical optical properties. Similarly, flip-flops between the N-V center triplet spins and the $g=2$ doublet spins are detectable by the microwave recovery experiment since the doublet species obviously has different optical properties. It is important to note that the microwave recovery rate directly reflects the energy-transfer rate, or the population relaxation rate, due to the flip-flop process. Thus the CR rate of 0.5×10^2 s^{-1} obtained from the microwave recovery experiment is a mean spin-flipping rate of one spin belonging to subensemble I by the flip-flops with spins belonging to subensemble II. It is noted that, since subensemble I contains less spins than subensemble II by a factor of $\frac{1}{3}$, the flip-flop rate between two spins belonging to subensemble I must be slower than 0.5×10^2 s^{-1}, although it is not detectable by the microwave recovery experiment (assuming there is no inhomogeneity in the optical properties within subensemble I). Similarly, the flip-flop rate of one spin in subensemble II must be of the order of 0.5×10^2 s^{-1}.

Now the CR effects on the spin-echo decay rates are considered. In case of the optical detection of spin coherence,[22–24] a $\pi/2-\tau-\pi-\tau-\pi/2$ microwave-pulse sequence is used for the observation of HED signals and a $\pi/2-\tau-\pi/2-T-\pi/2-\tau-\pi/2$ sequence for the observation of SED transients. In the case of SLD observation, a $\pi/2-\tau-\pi/2$ pulse sequence is used and the microwave polarization is phase shifted by 90° during the period between the two $\pi/2$ pulses in order to inhibit free induction decay.[23] The final $\pi/2$ pulse in the three experiments is a probe pulse for optical detection of the echoes.[22,23] As is usually the case, we define A spins as the probe spins which are excited by the microwave pulses and B spins as the nonexcited spins. The spin-dephasing rates observed in the spin-echo experiments are determined by the fluctuation frequency of the local field at each A-spin position. The local-field fluctuation at each A-spin position is produced by the spin flips of the surrounding spins. In the case of the SLD, the flipping of the probed A spin itself also contributes to the echo decay because the pure dephasing due to the local-field fluctuation is suppressed by the locking field. Consider the case when the two subensembles I and II are not resonant and the spin-echo experiment is performed for subensemble I. Since the Rabi frequency ($\cong3$ MHz) of the microwave is much smaller than the inhomogeneous width of subensemble I ($\cong15$ MHz), only a small fraction of the spins in subensemble I is excited (A spins). B spins, on the other hand, consist of the nonexcited spins in subensemble I and all the spins in subensemble II. Contributions of dipolar interactions between the N-V centers and $g=2$ doublet spins can be ignored because the spin-dephasing rate of N-V centers in crystal B is totally determined by the dipolar interaction between N-V centers themselves.[3] Also, the spin-lattice relaxation can be neglected at the present lattice temperature, as has been discussed in Sec. IV B. The flipping rate of each spin, as determined by dynamic dipolar interactions,[3,11] is 0.5×10^2 s^{-1} for each A or B spin or slower, as was discussed above. Since each A spin is surrounded by many B and A spins, the fluctuation frequency becomes the spin-flipping rate $k_{\rm fl}$ of each surrounding spin times the effective surrounding-spin number $N_{\rm eff}$. We define a distance $R_{\rm max}$ as the maximum distance between the probed A spin and a surrounding spin for which the spin flip still can contribute to the dephasing of the probed A spin. $N_{\rm eff}$ equals the number of spins inside a sphere of radius $R_{\rm max}$. Thus, although the local-field flipping rate is about 0.5×10^2 s^{-1} or slower, the spin-dephasing rate becomes much faster.

The difference between the HED and SED rates is explained by a difference in $R_{\rm max}$. Relatively speaking, only the larger local-field fluctuations contribute to SED. Accordingly, $R_{\rm max}$ becomes smaller in the case of SED because only the spin flips of nearby spins give rise to the larger fluctuations. Thus $N_{\rm eff}$ becomes smaller for SED, and the SED rate becomes smaller than the HED rate. In the SED experiment, $1/(2\tau)$ roughly determines the minimum fluctuation of the resonance frequency that contributes to the spin dephasing,[8,24,25] where τ is the time separation between the first two $\pi/2$ pulses. Since the SED experiment in Ref. 3 was performed with $\tau=3.0$ μs, only resonance-frequency fluctuations larger than about 150 kHz contribute to the SED decay. In this case $R_{\rm max}$ becomes about 70 Å. The observed SED decay rate of 1.3×10^3 s^{-1} implies that $N_{\rm eff}\cong20$ since $k_{\rm fl}\cong0.5\times10^2$ s^{-1}. Thus 20 N-V centers exist in a sphere of radius 70 Å, which corresponds to a spin density of about 1×10^{19} cm^{-3}, which agrees with the nitrogen impurity concentration of 10^{18}–10^{19} cm^{-3} in sample B.[25] In the case of HED, $N_{\rm eff}$ is estimated to be about 200 from the observed HED rate of 1.3×10^4 s^{-1}. Using the latter value, the minimum resonance-frequency fluctuation that contributes to the HED is estimated to be about 15 kHz. Similarly, the minimum resonance-frequency fluctuation that contributes to the SLD is roughly determined[23] by $\nu_1/2$, where ν_1 is the Rabi frequency corresponding to the microwave locking field. Since $\nu_1\cong3$ MHz in the experiment reported in Ref. 3, the minimum fluctuation for the SLD becomes about 1.5 MHz, which corresponds to $N_{\rm eff}\cong2$. Thus only the nearest few surrounding spins

contribute to the SLD signal, and the SLD rate becomes two orders of magnitude smaller than the HED rate, as actually observed in the experiment, the observed SLD rate being 2.4×10^2 s^{-1}.

Finally, the CR effects on the spin-echo decay rates are considered. When the two subensembles I and II are resonant, the microwave pulses excite spins of both subensembles. Thus the A spins include spins in subensemble II as well as spins in subensemble I. In analogy to the case of no CR, the dephasing rate of A spins is determined by the fluctuation frequency of the local field at each A-spin site, $k_{\rm fl}\times N_{\rm eff}$. The difference in the case of no CR is that $k_{\rm fl}$ is enhanced because of the CR between subensembles I and II. Thus, although the enhancement of the flip rate $k_{\rm fl}$ due to CR is only on the order of 10^2 s^{-1}, this enhancement results in one or two orders larger enhancement in the spin-echo decay rate depending on the value of $N_{\rm eff}$. In conclusion, a consistent picture can be given for the influence of CR on the spin dynamics probed in the microwave recovery and spin coherent transient measurements, respectively.

VI. CONCLUSIONS

At zero magnetic field, the microwave recovery transients observed for the N-V center in diamond can be fitted to a biexponential, which is characterized by two decay rate constants λ_+ and λ_- [cf. Eq. (26)]. The extrapolated value of λ_+ in the limit of zero laser excitation power is finite, while λ_- is extrapolated to zero [Fig. 5(a)]. This agrees with the analysis of the triplet-state kinetics in Sec. II A, taking CR effects into account. The extrapolated value of λ_+ represents the rate for CR between the two subensembles I and II. The estimated CR rate is $W=(0.2\pm0.3)\times10^2$ s^{-1}. Subensemble I also takes part in CR with an ensemble of $g=2.00$ doublet spins when a magnetic field of 514 G is applied along the [111] crystallographic axis. In this magnetic field, the microwave recovery of subensemble I becomes faster (Fig. 7), and the CR rate is estimated to be $W=(9.1\pm1.4)\times10^2$ s^{-1}. The CR dynamics as determined from the microwave recovery experiments is representative of the mean flip-flop rate of each spin within the optically excited subensemble. The CR effects observed in the spin coherence experiments reported elsewhere[3,4] are representative of the local-field fluctuations at the probed spin site and not of the flip-flop rate of the probe spin itself.

ACKNOWLEDGMENTS

This work was supported in part by the Netherlands Foundation for Chemical Research (SON) with financial aid from the Netherlands Organization for Scientific Research (NWO). One of the authors (I.H.) was supported in part by the Japanese Ministry of Education for his stay at the University of Amsterdam.

*Permanent address: Physics Department, Shimane University, Matsue 690, Japan.

[1]N. Bloembergen, S. Shapiro, P. S. Pershan, and J. O. Artman, Phys. Rev. **114**, 445 (1959).
[2]C. P. Slichter, *Principles of Magnetic Resonance,* 3rd ed. (Springer, Berlin, 1990).
[3]E. van Oort and M. Glasbeek, Phys. Rev. B **40**, 6509 (1989).
[4]E. van Oort and M. Glasbeek, Chem. Phys. **152**, 365 (1991).
[5]J. H. N. Loubser and J. H. van Wyk, Diamond Res. **11**, 4 (1977).
[6]J. H. N. Loubser and J. H. van Wyk, Rep. Prog. Phys. **41**, 1202 (1978).
[7]J. Walker, Rep. Prog. Phys. **42**, 1605 (1979).
[8]E. van Oort, N. B. Manson, and M. Glasbeek, J. Phys. C **21**, 4385 (1988).
[9]N. R. S. Reddy, N. B. Manson, and E. R. Krausz, J. Lumin. **38**, 46 (1987).
[10]D. A. Redman, S. Brown, R. H. Sands, and S. C. Rand, Phys. Rev. Lett. **67**, 3420 (1991).
[11]I. Hiromitsu, J. Westra, and M. Glasbeek, Phys. Rev. B **46**, 5303 (1992).
[12]H. Yoshida, D. Feng, and L. Kevan, J. Chem. Phys. **55**, 4924 (1973).
[13]W. M. Pitts and M. A. El-Sayed, Chem. Phys. **25**, 315 (1977).
[14]A. T. Collins, M. F. Thomaz, and M. I. B. Jorge, J. Phys. C **16**, 2177 (1983).
[15]J. Westra, R. Sitters, and M. Glasbeek, Phys. Rev. B **45**, 5699 (1992).
[16]M. Glasbeek and R. Hond, Phys. Rev. B **23**, 4220 (1981).
[17]E. van Oort and M. Glasbeek, Appl. Magn. Res. **2**, 291 (1991).
[18]W. V. Smith, P. P. Sorokin, I. L. Gelles, and G. J. Lasher, Phys. Rev. **115**, 1546 (1959).
[19]R. J. Cook and D. H. Whiffen, Proc. R. Soc. London A **295**, 99 (1966).
[20]J. H. N. Loubser and L. du Preez, Br. J. Appl. Phys. **16**, 457 (1965).
[21]R. Hond and M. Glasbeek, Phys. Rev. B **26**, 427 (1982).
[22]W. G. Breiland, C. B. Harris, and A. Pines, Phys. Rev. Lett. **30**, 158 (1973).
[23]C. B. Harris, R. L. Schlupp, and H. Schuch, Phys. Rev. Lett. **30**, 1019 (1973).
[24]W. B. Mims, in *Electron Paramagnetic Resonance,* edited by S. Geschwind (Plenum, New York, 1972), p. 263.
[25]E. van Oort, Ph.D. thesis, University of Amsterdam, 1990.